Magnetic Hofstadter butterfly and its topologically quantized Hall conductance

Manisha Arora and Sankalpa Ghosh
Department of Physics, Indian Institute of Technology Delhi, New Delhi 110016, India

(Received 7 July 2018; published 17 October 2018)

The energy spectrum of massless Dirac fermions in graphene under two-dimensional periodic magnetic modulation with square-lattice symmetry is calculated. We show that the translation symmetry of the problem is similar to that of the Hofstadter or Thouless–Kohmoto–Nightingale–den Nijs problem, and in the weak-field limit the tight-binding energy eigenvalue equation is indeed given by the Harper-Hofstadter Hamiltonian. We show that due to its magnetic translational symmetry the Hall conductivity can be identified as a topological invariant and hence quantized. We thus extend the idea of topologically quantized Hall conductance to a two-dimensional electron system under periodic magnetic modulation. Finally, we indicate possible experimental systems where this may be verified.

DOI: 10.1103/PhysRevB.98.155425

I. INTRODUCTION

The integer quantum Hall effect, one of the most fascinating phenomena in condensed-matter physics and beyond, shows extremely precise quantization of magnetotransport (Hall conductivity) in a two-dimensional electron gas (2DEG) placed in a transverse magnetic field. It was first discovered in a system with nonrelativistic dispersion [1–4] (silicon metal-oxide-semiconductor field-effect transistor and semiconductor heterostructure) and subsequently in a 2DEG with relativistic dispersion [5,6] realized in graphene.

In a seminal paper Thouless, Kohmoto, Nightingale, and den Nijs (TKNN) [7] identified this quantized Hall conductance of a 2DEG in a transverse magnetic field with a strong periodic potential [8] with a topological invariant [9] called the first Chern number defined in the space of Bloch vectors. This remarkable idea not only explained the robust quantization of a transport quantity but fundamentally modified the conventional understanding of the band structure of transport. This idea was further significantly generalized when Haldane [10] showed that such topological quantization of Hall conductivity can be achieved for a fully filled band even in the absence of a net magnetic field, leading to anomalous quantum Hall effect (AQHE). Haldane's seminal work was further generalized in systems without any external magnetic field, which respect time-reversal symmetry [11,12] and led to the discovery of present-day topological insulators [13].

This paper considers a two-dimensional gas of massless Dirac fermions with relativistic dispersion, the charge carriers in monolayer graphene, in the presence of a periodically modulated transverse magnetic field. We show that such magnetic field is composed of two parts. One part corresponds to a uniform field, like that in a prototype quantum Hall system. The other part gives a periodic modulation which has zero net flux through each unit cell. Thus, the second part gives a flux condition qualitatively similar to that in the Haldane's problem [10], leading to the AQHE, but realized in a different lattice geometry than Haldane's construction. Subsequently, we write the resulting vector potential as a combination of the usual symmetric gauge vector potential for a uniform transverse field and a periodic vector potential for the modulated part, whose form we also explicitly construct. This decomposition enables us to identify that the magnetic translation operator [14–16] for this problem is same as that in the TKNN [7] problem.

This has interesting consequences. The corresponding Hamiltonian is a perturbed form of the Hamiltonian used in the classic Hofstadter problem [8]. However, here the periodicity comes entirely from magnetic modulation. We therefore address this as a magnetic Hofstadter problem. In the tight-binding approximation and in the weak-field limit we show that the problem is indeed the Hofstadter-Harper equation. We analyze its spectrum. Finally, the properties of the magnetic Bloch functions are used to show that the Hall conductivity stays quantized as in the TKNN problem and can be identified with the Chern number of a filled band. Thus, our decomposition of the magnetic field profile allows us to show the topological quantization of Hall conductivity for a generic magnetically modulated 2DEG.

The effect of periodic magnetic modulation in one [17–19] and two dimensions [20–22] on a 2DEG was considered previously in a number of papers. They mostly explored the resulting band structure [17,18] and the perturbation of Landau levels (LLs) formed in a uniform magnetic field. Our decomposition of a general periodic magnetic modulation and the identification of the unique magnetic translation symmetry for a large class of Hamiltonians not only provide a unifying theoretical framework for these previous studies but also establish a connection between the conventional quantum Hall effect and the AQHE espoused in Haldane-like models. We conclude the paper by indicating some physical systems where this prediction can be put to experimental test.

II. THE MODEL

We consider the charge carriers in monolayer graphene in a transverse periodic magnetic field modulation (Fig. 1) given by

$$B\hat{z} = \left[B_2 + (B_1 - B_2)\sum_{m,n}\Theta(R^s - r_{mn})\right]\hat{z} \tag{1}$$

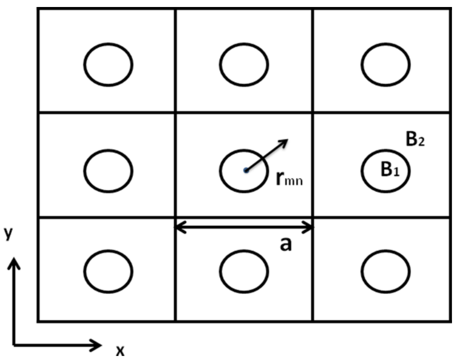

FIG. 1. Monolayer graphene under a two-dimensional magnetic field array with inside circular regions with radius R_s having $B_1\hat{z}$ and that of outside regions having $B_2\hat{z}$.

in the $\boldsymbol{k}\cdot\boldsymbol{p}$ representation, described by the massless Dirac Hamiltonian

$$\hat{H} = v_F(\boldsymbol{\sigma}\cdot\boldsymbol{\Pi}), \tag{2}$$

where $\boldsymbol{\Pi} = \boldsymbol{p} + \frac{e\boldsymbol{A}}{c}$ is the canonical momentum operator, with $\boldsymbol{A}$ being the vector potential for field (1). R^s is the radius of the circular region within each unit cell, $\boldsymbol{r}_{mn} = \boldsymbol{r} - \boldsymbol{R}_{mn}$, with $\boldsymbol{r} = x\hat{\boldsymbol{x}} + y\hat{\boldsymbol{y}}$. The lattice vector $\boldsymbol{R}_{mn} = ma\hat{\boldsymbol{x}} + na\hat{\boldsymbol{y}}$, and

$$\Theta(R^s - r_{mn}) = \begin{cases} 1 \ \text{if} \ r_{mn} \leqslant R^s, \\ 0 \ \text{if} \ r_{mn} > R^s, \end{cases} \tag{3}$$

with $m,n \in I(-N_{\max}, +N_{\max})$ and a being the lattice constant. It is assumed that the lattice constant a is much larger than the carbon-carbon bond length in a graphene honeycomb lattice so that a continuum model is justified. Apart from this, the step function modeling can be justified by assuming that the magnetic field gradient at the step is much sharper than the typical Fermi wavelength of the electron [17,23–25]. Such two-dimensional periodic modulation corresponds to that of a square lattice and can be made using nanolithographic techniques [26,27].

A. Decomposition

Using Fourier's theorem, the periodic magnetic field profile given by Eq. (1) can be written as

$$\boldsymbol{B} = \sum_{\boldsymbol{G}} \boldsymbol{B}_{\boldsymbol{G}} e^{i\boldsymbol{G}\cdot\boldsymbol{r}} = \boldsymbol{B}_0 + \sum_{\boldsymbol{G}\neq 0} \boldsymbol{B}_{\boldsymbol{G}} e^{i\boldsymbol{G}\cdot\boldsymbol{r}}. \tag{4}$$

Here $\boldsymbol{G}$ is the reciprocal lattice vector of the periodic lattice, and $\boldsymbol{B}_0 = \boldsymbol{B}_u$ is the uniform magnetic field and is given by the spatial average of the field given in Eq. (1). The residual periodic field is defined as $\boldsymbol{B}_p = \sum_{\boldsymbol{G}\neq 0} \boldsymbol{B}_{\boldsymbol{G}} e^{i\boldsymbol{G}\cdot\boldsymbol{r}}$, which satisfies $\nabla\cdot\boldsymbol{B}_p = 0$ with net flux through the unit cell due to $\boldsymbol{B}_p$ being zero (for details see Appendix A). This decomposition remains valid even for an arbitrary periodic modulation and is a consequence of the Fourier series decomposition. Consequently, if we apply uniform magnetic field $-\boldsymbol{B}_u$ to this system, under suitable conditions, it can realize a Haldane-like model [28,29] which shows AQHE. This may be contrasted with lattice models that explicitly contain terms responsible for the quantum Hall effect (QHE) and the quantum spin Hall effect [30] to demonstrate the connection between these two effects.

Now, following [31], it can be shown that there is a corresponding periodic vector potential for the residual periodic field $\boldsymbol{B}_p$. Accordingly, we can decompose the magnetic field and corresponding vector potential in uniform and periodic parts as

$$B\hat{z} = B_u\hat{z} + B_p\hat{z}, \quad \boldsymbol{A}(\boldsymbol{r}) = \boldsymbol{A}_u(\boldsymbol{r}) + \boldsymbol{A}_p(\boldsymbol{r}),$$

with

$$B_u = \left[B_2 + \frac{(B_1 - B_2)\pi(R^s)^2}{a^2}\right]$$

$$B_p = \left\{\sum_{m,n}[(B_1 - B_2)\theta(R^s - r_{mn})] - \frac{(B_1 - B_2)\pi(R^s)^2}{a^2}\right\}, \tag{5}$$

$$\boldsymbol{A}_u(\boldsymbol{r}) = \frac{1}{2}\boldsymbol{B}_u \times \boldsymbol{r},$$

$$\boldsymbol{A}_p(\boldsymbol{r}) = \frac{1}{2}\sum_{m,n}\left[\left(B_p^{mn}\hat{z}\right) \times (r_{mn}\hat{\boldsymbol{r}}_{mn})\right], \tag{6}$$

where

$$B_p^{mn} = \begin{cases} \left[(B_1 - B_2) - \frac{(B_1 - B_2)\pi(R^s)^2}{a^2}\right]\Theta(R^s - r_{mn}) \ \text{if} \ r_{mn} \leqslant R^s, \\ (B_2 - B_1)\frac{\pi(R^s)^2}{Na^2}\Theta(r_{mn} - R^s) \quad \text{otherwise}. \end{cases} \tag{7}$$

$\boldsymbol{A}_u(\boldsymbol{r})$ is in the Symmetric Gauge form. To construct $\boldsymbol{A}_p(\boldsymbol{r})$, we considered the single-unit magnetic field profile $[\frac{B_2}{N} + (B_1 - B_2)\Theta(R^s - r_{m,n})]\hat{z}$ for a specific (m,n). The vector potential for such a field can be found in the azimuthal gauge using Stoke's law. Superposing such units for all possible (m,n) and doing suitable gauge transformation, one gets $\boldsymbol{A}_p(\boldsymbol{r})$ (for details see Appendix A).

B. Modified Hofstadter-Harper equation

With the canonical momentum operator now defined as $\boldsymbol{\Pi} = \boldsymbol{p} + \frac{e}{c}(\boldsymbol{A}_u + \boldsymbol{A}_p)$, the eigenvalue equation for the Hamiltonian in (2), is rewritten as

$$v_F\begin{bmatrix} 0 & \Pi_x - i\Pi_y \\ \Pi_x + i\Pi_y & 0 \end{bmatrix}\begin{bmatrix} \psi^a_{k_x,k_y} \\ \psi^b_{k_x,k_y} \end{bmatrix} = E\begin{bmatrix} \psi^a_{k_x,k_y} \\ \psi^b_{k_x,k_y} \end{bmatrix}. \tag{8}$$

Here the periodic vector potential $\boldsymbol{A}_p$ has the periodicity of the square-lattice magnetic modulation. Thus, the magnetic translation operator $M_{\boldsymbol{R}}$ corresponding to $\boldsymbol{\Pi}$ is the same as the magnetic translation operator [14–16] of an electron in the periodic scalar potential of a square lattice and uniform transverse magnetic field. Explicitly,

$$M_{\boldsymbol{R}} = \exp\left[\frac{i}{\hbar}\boldsymbol{R}\cdot\left(\boldsymbol{p} - \frac{e\boldsymbol{A}_u}{c}\right)\right]. \tag{9}$$

We note that by construction $[\boldsymbol{p} + \frac{e}{c}\boldsymbol{A}_u, M_{\boldsymbol{R}}] = 0$. Since the periodic part of the vector potential $\boldsymbol{A}_p(\boldsymbol{r}+\boldsymbol{R}) = \boldsymbol{A}_p(\boldsymbol{r})$, we have $[\boldsymbol{A}_p, M_{\boldsymbol{R}}] = 0$. Thus, the Hamiltonian in (2) or in (8) commutes with $M_{\boldsymbol{R}}$, and they have simultaneous eigenstates which are magnetic Bloch functions [32]. This result depends on only the periodicity of $\boldsymbol{A}_p$ and not on the explicit form (6). Since the existence of a periodic vector potential is guaranteed for a periodic magnetic field that gives zero flux through each unit cell [31] and any periodic magnetic field can be decomposed in a uniform and periodic part satisfying the zero-flux condition, the above result implies the existence of the magnetic translational symmetry for a large class of Hamiltonians. This is one of the major findings of this work (see Appendix A). The significance of this result is that it is now possible to obtain the spectral properties as well as, using TKNN approach, the transport properties for the quasiparticles described by the Hamiltonian (2).

To obtain the spectrum we use the standard procedure of decoupling Eq. (8) and get the eigenvalue equations for each sublattice. This becomes

$$\hat{H}_G(x,y)\psi^{a,b}_{\boldsymbol{k}}(x,y) = E^2\psi^{a,b}_{\boldsymbol{k}}(x,y), \tag{10}$$

with

$$\hat{H}_G = v_F^2\left[\left(p + \frac{e}{c}A_u\right)^2 + V_p(\boldsymbol{r}) + V_{np}(\boldsymbol{r})\right], \tag{11}$$

where $V_p(\boldsymbol{r}) = \frac{e^2}{c^2}A_p^2 + \frac{2e}{c}\boldsymbol{A}_p\cdot\boldsymbol{p} + \hbar\frac{e}{c}(B_u + B_p)$ and $V_{np}(\boldsymbol{r}) = 2\frac{e^2}{c^2}\boldsymbol{A}_u\cdot\boldsymbol{A}_p$, such that $V_{np}(\boldsymbol{r}+\boldsymbol{R}) = V_{np}(\boldsymbol{r}) + 2\frac{e^2}{c^2}\boldsymbol{A}_u(\boldsymbol{R})\cdot\boldsymbol{A}_p(\boldsymbol{r})$ defines the nonperiodic part of the potential. The Hamiltonian H_G is equivalent to the Harper-Hofstadter Hamiltonian [8,33], but with the nonperiodic potential $V_{np}(\boldsymbol{r})$.

Since the eigenfunctions are the magnetic Bloch functions, namely, the eigenstates of $M_{\boldsymbol{R}}$ in Eq. (9), to write the eigenvalue equation (10) in a tight-binding form we expand them in terms of localized Wannier functions in the presence of uniform transverse magnetic field $\boldsymbol{B}_u$ [34,35]:

$$\psi^a_{\boldsymbol{k}} = \sum_i g(\boldsymbol{R}_i)\exp\left(-i\frac{e\boldsymbol{A}_u\cdot\boldsymbol{R}_i}{\hbar c}\right)w_0(\boldsymbol{r}-\boldsymbol{R}_i). \tag{12}$$

To simplify the problem further we set the condition $|\frac{ea^2}{\hbar c}(B_u + B_p)| \ll 1$. For $B_p = 0$, this condition translates into $a \ll l_{B_u}$, ($l_{B_u} = \sqrt{\frac{\hbar c}{eB_u}}$), implying weak and slowly varying magnetic field [34,36]. This type of condition is used in lattice gauge theory calculation [37]. Here using this, we can write the eigenvalue equation (10) in the form of a discrete Schrödinger equation which takes the form of the Hofstadter-Harper equation (see details in Appendix B):

$$\begin{aligned}\epsilon g(m,n) &= e^{\frac{iea}{\hbar c}(A_{ux}+A_{px})}g(m+1,n)\\ &\quad + e^{-\frac{iea}{\hbar c}(A_{ux}+A_{px})}g(m-1,n)\\ &\quad + e^{\frac{iea}{\hbar c}(A_{uy}+A_{py})}g(m,n+1)\\ &\quad + e^{-\frac{iea}{\hbar c}(A_{uy}+A_{py})}g(m,n-1)\\ &\quad - \left[\frac{ea^2}{\hbar c}(B_u+B_p)+4\right]g(m,n),\end{aligned} \tag{13}$$

with $\epsilon = \frac{-E^2a^2}{v_F^2\hbar^2}$.

It may be pointed out that in absolute value the magnetic field may still be substantially high and can provide a substantial gap in the energy spectrum if the lattice separation is of the order of ~100 nm, which is possible within current technology [27].

C. Energy spectrum

The magnetic translation operator in Eq. (9) forms a magnetic translation group satisfying the algebra [38]

$$\begin{aligned}M_{\boldsymbol{R}_1}M_{\boldsymbol{R}_2} &= \exp\left(\frac{2\pi i}{\phi_0}\phi\right)M_{\boldsymbol{R}_2}M_{\boldsymbol{R}_1},\\ M_{\boldsymbol{R}_1}M_{\boldsymbol{R}_2} &= \exp\left(\frac{\pi i}{\phi_0}\phi\right)M_{\boldsymbol{R}_1+\boldsymbol{R}_2},\end{aligned} \tag{14}$$

where $\phi = \boldsymbol{B}_u\cdot(\boldsymbol{R}_1\times\boldsymbol{R}_2) = \frac{p}{q}\phi_0$ is chosen as a rational number of flux quanta that pass through a unit cell. This defines the magnetic unit cell $\boldsymbol{R}' = m(q)a\hat{\boldsymbol{x}} + na\hat{\boldsymbol{y}}$ such that $B_uqa^2 = p$, an integer. This gives

$$B_2 = [(p/q)\phi_0 - B_1\pi Rs^2]/(a^2 - \pi Rs^2). \tag{15}$$

The corresponding magnetic Brillouin zone (MBZ) is defined as $0 \leqslant k_x \leqslant \frac{2\pi}{qa}$ and $0 \leqslant k_y \leqslant \frac{2\pi}{a}$. If the redefined magnetic lattice has N_q points along the x axis and N_y points along the y axis, then by construction $N_qq = 2N_{\max} + 1 = N_y$.

The two ends of the lattice along the x axis and y axis are connected by $\boldsymbol{R}_x = qN_qa\hat{\boldsymbol{x}}$ and $\boldsymbol{R}_y = N_ya\hat{\boldsymbol{y}}$, respectively. To solve the eigenvalue problem one can use the condition along the x and y axes as $M_{\boldsymbol{R}_x}\psi^a_{\boldsymbol{k}}(x,y) = \psi^a_{\boldsymbol{k}}(x,y)$ and $M_{\boldsymbol{R}_y}\psi^a_{\boldsymbol{k}}(x,y) = \psi^a_{\boldsymbol{k}}(x,y)$, where $\psi^a_{\boldsymbol{k}}(x,y)$ are the eigenfunctions of H_G. It can be checked [38,39] that if the number of fluxes through each unit cell is a rational number $\frac{p}{q}$, such a boundary condition can be satisfied.

With the relation (15) and the mentioned boundary conditions we numerically solve Eq. (13). The results are plotted in Figs. 2 and 3. In Fig. 2, keeping $B_1 = B_u + B_p$ fixed, we plot the dimensionless energy $\pm\sqrt{-\epsilon}$ for the particle-hole spectrum [40] as a function of $\frac{p}{q}$ for two different values of B_1. The increase in the gap between the particle and hole spectrum with increasing B_1 is clearly visible. Figure 3, on the other hand, plots the same energy spectrum, but keeping B_2 fixed, for two representative values of B_2. For each value of B_2, in accordance with Eq. (15), B_1 varies with $\frac{p}{q}$ as we move along the horizontal axis. This causes a variable gap between the particle and hole spectrum as $\frac{p}{q}$ changes. After discussing the spectrum of the Hamiltonian in Eq. (8), we shall now evaluate the Hall conductance of the system and connect it to the spectrum.

III. TOPOLOGICAL QUANTIZATION OF HALL CONDUCTANCE AND THE DIOPHANTINE EQUATION

The eigenfunctions of the Hamiltonian (8) can also be written in the Bloch form as

$$\begin{bmatrix}\psi^a_{k_x,k_y}\\ \psi^b_{k_x,k_y}\end{bmatrix} = e^{i\boldsymbol{k}\cdot\boldsymbol{r}}\begin{bmatrix}u^a_{k_x,k_y}\\ u^b_{k_x,k_y}\end{bmatrix}. \tag{16}$$

We define

$$u'_{k_x,k_y} = \begin{bmatrix}u^a_{k_x,k_y}\\ u^b_{k_x,k_y}\end{bmatrix}.$$

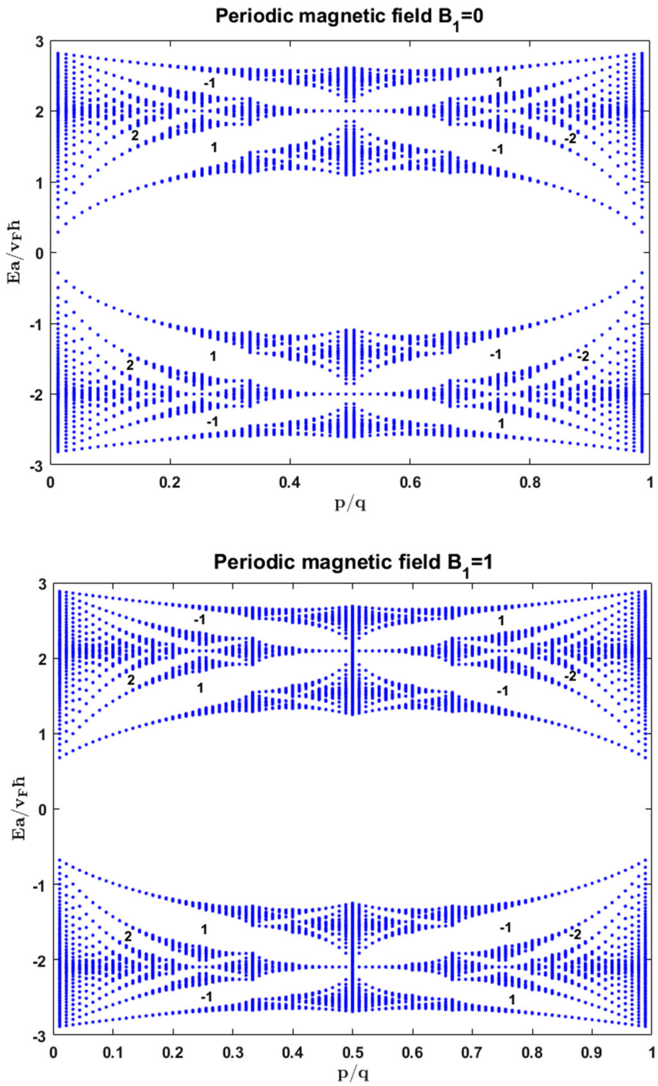

FIG. 2. Dimensionless energy $\frac{Ea}{\hbar v_F}$ versus $\frac{p}{q}$ [Eq. (13)] with $B_1 = 0$ (top) and $B_1 = 1$ (bottom). The values of p satisfy $1 \leqslant p \leqslant q-1$, $a = 0.25$, and $R^s = 0.0825$.

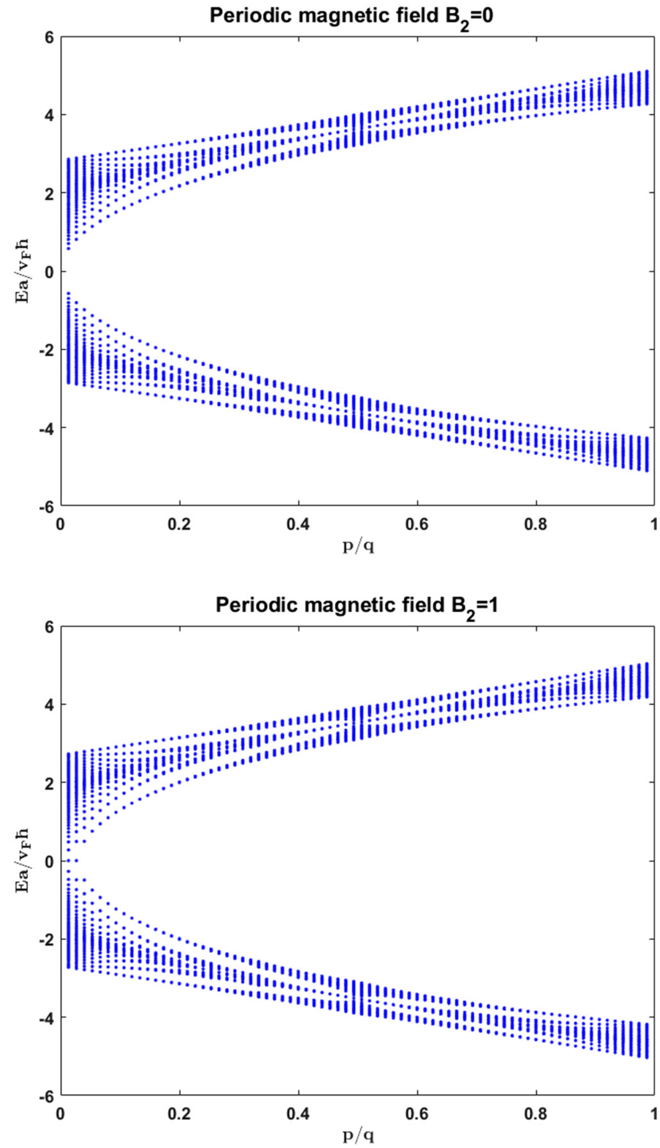

FIG. 3. Dimensionless energy $\frac{Ea}{\hbar v_F}$ versus p/q [Eq. (13)] with $B_2 = 0$ (top) and $B_2 = 1$ (bottom). Other parameters are the same as in Fig. 2.

Since $B_u \neq 0$, the commutation relation (14) implies that $u^{a,b}_{k_x,k_y}$ must have zeros inside a magnetic unit cell and must have the structure $u^{a,b}_{k_x,k_y} = |u^{a,b}_{k_x,k_y}(x,y)| \exp[i\theta^{a,b}_{k_x,k_y}(x,y)]$ [41]. These functions can be found by solving the Schrödinger equation $\hat{H}(k_x,k_y)u'^{n_b}_{k_x,k_y} = E^{n_b}u'^{n_b}_{k_x,k_y}$, where n_b is the band index. Following TKNN [7], the Hall conductance calculated through the Kubo formula in the linear-response regime for a completely filled band (the band index is omitted due to a single band) can therefore be obtained as

$$\sigma_{xy} = \frac{e^2}{h}\frac{1}{2\pi i}\int d^2k[\nabla_{\boldsymbol{k}} \times \hat{\boldsymbol{A}}(k_x,k_y)]_3, \tag{17}$$

where the integration is over the MBZ and

$$\hat{\boldsymbol{A}}(k_x,k_y) = \int d^2r u'^{*}_{k_x,k_y}\nabla_{\boldsymbol{k}} u'_{k_x,k_y} \tag{18}$$

is the Berry connection defined over such a MBZ. Since the two points $k_x = 0$ and $k_x = \frac{2\pi}{qa}$ (or $k_y = 0$ and $k_y = \frac{2\pi}{a}$) are equivalent, the MBZ has the topology of a torus. The phase of the wave function cannot be uniquely determined in the MBZ because of the existence of zeros of such a wave function. This leads to a finite value of the above integral, and quantization of the Hall conductivity in this case gives

$$\sigma_{xy} = \frac{2e^2}{h}\sigma_H, \tag{19}$$

where σ_H is an integer. Here the factor of 2 comes from the sublattice degrees of freedom in single-layer graphene. Thus, if the Fermi energy lies in one of the gaps of the spectrum, the Hall conductivity is quantized in terms of an integer [7] relevant to the filled band lying below the Fermi energy. Perturbations like disorder, interactions, and the effect of the higher-order terms neglected in (13) can negate the above result only if the gap closes. Details of the calculation closely follow [41] and are summarized in Appendix C. We would like to mention that QHE with modified LLs can also occur in graphene under a one-dimensional periodic scalar potential due to the generation of additional Dirac points [42,43].

To relate the integers in Eq. (19) with the spectrum plotted in Fig. 2, we note that integration of the Berry connection $\hat{A}(k_x, k_y)$ gives the geometric phase change of the functions u'_{k_x,k_y} over the MBZ. Following [44,45], it is possible to show that the corresponding magnetic Bloch functions satisfy the boundary condition (see Appendix D)

$$\psi_{k_x+\frac{b_1}{q},k_y} = \psi_{k_x,k_y},\ \ \psi_{k_x,k_y+b_2} = e^{i\sigma_H k_x q a}\psi_{k_x,k_y}, \tag{20}$$

where $\boldsymbol{b}_1 = \frac{2\pi}{a}\hat{\boldsymbol{x}}$ and $\boldsymbol{b}_2 = \frac{2\pi}{a}\hat{\boldsymbol{y}}$ are the reciprocal lattice vectors. This condition must be consistent with the group properties defined in Eqs. (14) of the magnetic translation operator, given in Eq. (9), leading to

$$M_{a\hat{\boldsymbol{y}}} M_{a\hat{\boldsymbol{x}}} \psi_{\boldsymbol{k}} = e^{i(\boldsymbol{k}+\frac{p}{q}\boldsymbol{b}_2).a\hat{\boldsymbol{y}}} M_{a\hat{\boldsymbol{x}}} \psi_{\boldsymbol{k}}, \tag{21}$$

where $M(a\hat{\boldsymbol{x}})\psi_{\boldsymbol{k}}$ depicts the eigenfunction of $M(a\hat{\boldsymbol{y}})$ with the eigenvalue $e^{i(\boldsymbol{k}+\frac{p}{q}\boldsymbol{b}_2)\cdot a\hat{\boldsymbol{y}}}$. In the same way $M_{a\hat{\boldsymbol{x}}}\psi_{\boldsymbol{k}}, \ldots, M_{(q-1)a\hat{\boldsymbol{x}}}\psi_{\boldsymbol{k}}$ all have different eigenvalues for $M_{a\hat{\boldsymbol{y}}}$ but the same eigenvalue for the Hamiltonian. This leads to a q-fold degeneracy for each energy eigenvalue. The algebraic relation that connects the boundary condition in Eq. (20) to relation (21) connects $\frac{p}{q}$ to the integer σ_H through the famous Diophantine equation

$$\mu q + \sigma_H p = 1. \tag{22}$$

This equation is equivalent to the equation given by TKNN [7] for square-lattice systems to calculate the Chern numbers associated with σ_H for the rth gap in a Landau level as $r = s_r q + t_r p$. Under the constraint $|t_r| \leqslant q/2$ this yields a unique solution (s_r, t_r). Here $\sigma_H = t_r - t_{r-1}$, and $\mu = s_r - s_{r-1}$ [46]. In our system with square-lattice magnetic modulation using the same method we calculate t_r for a few such swaths in Fig. 2.

IV. SUMMARY

We predicted the topological quantization of Hall conductivity for massless Dirac fermions in monolayer graphene under a generic two-dimensional periodic magnetic modulation. The results can be extended to a nonrelativistic 2DEG. Similar topological quantization in non-Bravais-type magnetic modulation in the hexagonal lattice [47], the effect of additional periodic electrostatic potential and (in)commensuration between two types of periodicities [8,48,49], and the bulk and edge correspondence in such a system [4,50] are some possible directions for further investigations. Periodic two-dimensional magnetic modulation was already created for a 2DEG in GaAs-AlGaAs heterojunctions using ferromagnetic dysprosium dots [26]. The van der Waals heterostructure of monolayer graphene [51] with layered magnetic materials such as the transition-metal phosphorus trisulfide [52] may also realize similar modulations.

ACKNOWLEDGMENTS

We acknowledge helpful discussions and correspondence with S. Gupta, S. Shringarpure, M. Sharma, and I. Dana. M.A. is supported by a MHRD fellowship.

APPENDIX A: PROOFS RELATED TO $B_p\hat{z}$ AND A_p

The flux due to $B_p\hat{\boldsymbol{z}}$ in Eq. (5) through a unit cell is

$$\begin{aligned}\int_{\text{unit cell}} B_p\hat{\boldsymbol{z}}\cdot d\boldsymbol{s} &= \frac{1}{a^2}\bigg[(B_1-B_2)\bigg(1-\frac{\pi Rs^2}{a^2}\bigg)\pi Rs^2 \\ &\quad - (B_1-B_2)\frac{\pi Rs^2}{a^2}(a^2-\pi Rs^2)\bigg] \\ &= 0.\end{aligned} \tag{A1}$$

To show that the condition (A1) is, in general, valid for a periodic magnetic field, we proceed as follows: For any general periodic magnetic field profile, using Fourier's theorem, we can write

$$\boldsymbol{B} = \sum_{\boldsymbol{G}} \mathbf{B}_{\boldsymbol{G}} e^{i\boldsymbol{G}\cdot\mathbf{r}} = \boldsymbol{B}_{\mathbf{0}} + \sum_{\boldsymbol{G}\neq 0} \boldsymbol{B}_{\boldsymbol{G}} e^{i\boldsymbol{G}\cdot\boldsymbol{r}}. \tag{A2}$$

Here $\boldsymbol{G}$ is the reciprocal lattice vector, and $\boldsymbol{B}_0 = \boldsymbol{B}_u$ is uniform and is the spatial average of the field $\boldsymbol{B}$. The residual part, $\sum_{\boldsymbol{G}\neq 0} \boldsymbol{B}_{\boldsymbol{G}} e^{i\boldsymbol{G}\cdot\boldsymbol{r}}$, is the periodic part (say, $\boldsymbol{B}_p$) that has the same periodicity as the original modulation. Hence, we can rewrite Eq. (A2) as

$$\boldsymbol{B} = \boldsymbol{B}_u + \boldsymbol{B}_p.$$

Now,

$$\int \boldsymbol{B}\cdot \mathbf{dS} = \int \boldsymbol{B}_u \cdot d\boldsymbol{S} + \int \boldsymbol{B}_p \cdot d\boldsymbol{S},$$

which leads to (A is the area of the two-dimensional plane)

$$\begin{aligned} B_u A &= B_u A + \int \boldsymbol{B}_p \cdot d\boldsymbol{S} \\ &\Rightarrow \int \boldsymbol{B}_p \cdot d\boldsymbol{S} = 0.\end{aligned}$$

Now, as

$$\boldsymbol{B}_p(\mathbf{r}+\boldsymbol{R}) = \boldsymbol{B}_p(\boldsymbol{r}),$$

this implies that the flux due to $\boldsymbol{B}_p$ is zero in each unit cell since it is identical in each unit cell. This fact along with $\nabla\cdot\boldsymbol{B}_p = 0$ confirms that a gauge can always be chosen such that a periodic vector potential (say, $\boldsymbol{A}_p$) for the field profile $\boldsymbol{B}_p$ is found [31]. Now whenever we pick any 2D periodic field profile, we need to calculate the explicit form of its $\boldsymbol{A}_p$ corresponding to $\boldsymbol{B}_p$.

The explicit construction of the profile of the vector potential $\boldsymbol{A}_p(\boldsymbol{r})$ for the present problem is given as follows: Consider the magnetic field profile

$$B_s\hat{z} = \bigg[\frac{B_2}{N} + (B_1-B_2)\Theta(R^s - r_{m,n})\bigg]\hat{z} \tag{A3}$$

depicted in Fig. 1. A superposition of such a magnetic field profile through summation over all allowed values of m, n will generate the magnetic field profile $\boldsymbol{B}$ given by Eq. (1).To evaluate the vector potential corresponding to $\boldsymbol{B}$, we first calculate

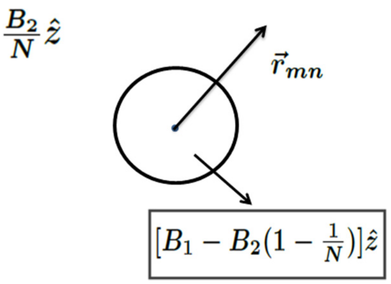

FIG. 4. Monolayer graphene under a single-unit magnetic field profile with the inside circular region having field $[B_1 - B_2(1 - \frac{1}{N})]\hat{z}$ and the outside region having $\frac{B_2}{N}\hat{z}$. The radius of the circular region is R^s.

the vector potential corresponding to $B_s\hat{z}$ given in Eq. (A3). Then we superpose all such vector potentials corresponding to different sets of (m,n). Now, the magnetic field profile in Fig. 4 suggests that it is possible to write the vector potential purely with an azimuthal component. Accordingly, we write

$$\int \frac{\boldsymbol{B}_s \cdot d\boldsymbol{S}}{\Phi_0} = \int \frac{\boldsymbol{A}_s \cdot d\boldsymbol{l}}{\Phi_0},$$

where $\boldsymbol{A}_s$ is the vector potential having only an azimuthal component. Here $\Phi_o = \frac{hc}{e}$. From the above equation we straightforwardly get

$$A_{s\theta} = \frac{c\phi(r)}{er}, \tag{A4}$$

where $\phi(r)$ is given as

$$\phi(r) = \begin{cases} \frac{e}{c}\left[\frac{B_2}{N}\frac{r^2}{2} + \frac{(B_1-B_2)r^2}{2}\right] & \text{if } r \leqslant R^s, \\ \frac{e}{c}\left[\frac{B_2}{N}\frac{r^2}{2} + \frac{(B_1-B_2)(R^s)^2}{2}\right] & \text{otherwise.}\end{cases}$$

It may be pointed out in cases like this [Eq. (A3)] where the magnetic field profile contains a step function, we adopted this technique based on Stoke's theorem to calculate the corresponding vector potential. For example, see Ref. [23].

Hence, from Eq. (A4), we can write

$$A_{s\theta}(r) = \begin{cases} \left[\frac{B_2}{N}\frac{r}{2} + \frac{(B_1-B_2)r^2}{2r}\right] & \text{if } r \leqslant R^s, \\ \left[\frac{B_2}{N}\frac{r}{2} + \frac{(B_1-B_2)(R^s)^2}{2r}\right] & \text{otherwise.}\end{cases}$$

From this, we find that for a given (m,n) the azimuthal component of the vector potential is given as

$$A_{mn} = \begin{cases} \left[\frac{B_2}{N}\frac{r_{mn}}{2} + \frac{(B_1-B_2)r_{mn}^2}{2r_{mn}}\right] & \text{if } r_{mn} \leqslant R^s, \\ \left[\frac{B_2}{N}\frac{r_{mn}}{2} + \frac{(B_1-B_2)(R^s)^2}{2r_{mn}}\right] & \text{otherwise,}\end{cases}$$

where r_{mn} and R^s are defined in the main text. Thus, the total vector potential for the field profile $\boldsymbol{B}$ can be written as

$$\boldsymbol{A}(\boldsymbol{r}) = \sum_{m,n}[(\boldsymbol{A}_{mn}\cdot\hat{\boldsymbol{x}})\hat{\boldsymbol{x}} + (\boldsymbol{A}_{mn}\cdot\hat{\boldsymbol{y}})\hat{\boldsymbol{y}}].$$

Since $B\hat{z} = B_u\hat{z} + B_p\hat{z}$, then up to a gauge choice the vector potential [say, $\boldsymbol{A}_{\text{rem}}(\boldsymbol{r})$] corresponding to $\boldsymbol{B}_p$ can be obtained as

$$\boldsymbol{A}_{\text{rem}}(\boldsymbol{r}) = \boldsymbol{A}(\boldsymbol{r}) - \boldsymbol{A}_u(\boldsymbol{r}),$$

where $\boldsymbol{A}_u = \frac{1}{2}(\boldsymbol{B}_u \times \boldsymbol{r})$ is given in the symmetric gauge. A straightforward but lengthy algebra involving various terms in the expression of $\boldsymbol{A}_{\text{rem}}(\boldsymbol{r}) = A_{\text{remx}}\hat{\boldsymbol{x}} + A_{\text{remy}}\hat{\boldsymbol{y}}$ shows that $\boldsymbol{A}_{\text{rem}}$ can be written as a superposition of a periodic term and another part $\boldsymbol{A}_{\text{rem}}^{\text{rest}}$, whose curl is zero. The second part can therefore be removed through a gauge transformation, and this leaves us with the expression for the periodic vector potential $\boldsymbol{A}_p(\boldsymbol{r})$ corresponding to $\boldsymbol{B}_p$, shown in Eq. (5).

More explicitly, we can write

$$\begin{aligned}\boldsymbol{A}_p(\boldsymbol{r}) &= \frac{1}{2}\sum_{m,n}\left[\left(B_p^{mn}\hat{z}\right)\times(\boldsymbol{r}-\boldsymbol{R}_{mn})\right] \\ &= \frac{1}{2}\sum_{m,n}\left[\left(B_p^{mn}\hat{z}\right)\times(r_{mn}\hat{\boldsymbol{r}}_{mn})\right] \\ &= \frac{1}{2}\sum_{m,n}\left(B_p^{mn}r_{mn}\right)\hat{\boldsymbol{\theta}}_{mn},\end{aligned} \tag{A5}$$

where B_p^{mn} is defined, in the main text, in Eq. (7), and we can show that $\nabla \times (\boldsymbol{A}_{\text{rem}} - \boldsymbol{A}_p) = 0$. Now, the periodicity of $\boldsymbol{A}_p(\boldsymbol{r})$ can be proved as follows: Rewrite $\boldsymbol{A}_p(\boldsymbol{r})$ from Eq. (6) as

$$\boldsymbol{A}_p(\boldsymbol{r}) = \frac{1}{2}\sum_{m,n}\left[\left(B_p^{mn}\hat{z}\right)\times(\boldsymbol{r}-\boldsymbol{R}_{mn})\right].$$

Now performing a lattice translation with vector $\boldsymbol{R} = la\hat{\boldsymbol{x}} + ka\hat{\boldsymbol{y}}$, we obtain

$$\boldsymbol{A}_p(\boldsymbol{r}+\boldsymbol{R}) = \frac{1}{2}\sum_{m'',n''}\left[\left(B_p^{m''n''}\hat{z}\right)\times(\boldsymbol{r}-\boldsymbol{R}_{m''n''})\right],$$

where $m'' = (m-l)$ and $n'' = (n-k)$ and the limits are $m'' = (-N_{\max} - l) : (N_{\max} - l)$ and $n'' = (-N_{\max} - k) : (N_{\max} - k)$. Thus,

$$\boldsymbol{A}_p(\boldsymbol{r}+\boldsymbol{R}) = \boldsymbol{A}_p(\boldsymbol{r}).$$

APPENDIX B: DERIVATION OF EQUATION (13) FROM EQUATION (10)

Discretization and implementation of the weak-magnetic-field condition are shown as follows: Consider the Taylor expansion

$$\psi(x+a) = \psi(x) + a\frac{\partial\psi(x)}{\partial x} + \frac{a^2}{2!}\frac{\partial^2\psi(x)}{\partial x^2} + \cdots.$$

For a slowly varying function, therefore,

$$a\frac{\partial\psi(x)}{\partial x} + \frac{a^2}{2!}\frac{\partial^2\psi(x)}{\partial x^2} \sim \psi(x+a) - \psi(x). \tag{B1}$$

Define the dimensionless variables and the functions in terms of them as

$$\bar{x} = \frac{x}{l_{Bu}}, \quad \phi(\bar{x}) = \psi(x), \tag{B2}$$

where ℓ_{B_u} is the magnetic length corresponding to the uniform magnetic field $B_u\hat{z}$. Now

$$\begin{aligned}\frac{\partial\psi(x)}{\partial x} &= \frac{1}{l_{Bu}}\frac{\partial\phi(\bar{x})}{\partial\bar{x}}, \\ \frac{\partial^2\psi(x)}{\partial x^2} &= \frac{1}{l_{Bu}^2}\frac{\partial^2\phi(\bar{x})}{\partial^2\bar{x}}.\end{aligned} \tag{B3}$$

Now using Eqs. (B2) and (B3) in Eq. (B1), we get

$$\frac{a}{l_{Bu}}\frac{\partial\phi(\bar{x})}{\partial\bar{x}}+\frac{1}{2!}\left(\frac{a}{l_{Bu}}\right)^2\frac{\partial^2\phi(\bar{x})}{\partial^2\bar{x}}=[\phi(\overline{x+a})-\phi(\bar{x})].$$

For $\frac{a}{l_{Bu}} \ll 1$ (for the uniform magnetic field case) [37], we can even neglect terms containing $(\frac{a}{l_{Bu}})^2$ and higher orders. Thus,

$$\frac{\partial\psi(x)}{\partial x}=\frac{\psi(x+a)-\psi(x)}{a}.$$

Rewriting the condition in terms of magnetic field, it reads $|\frac{ea^2B_u}{\hbar c}| \ll 1$, which is satisfied for a weak and slowly varying field. This condition can be extended for the case of

$$\left|\frac{ea^2B(\boldsymbol{r})}{\hbar c}\right| \ll 1, \tag{B4}$$

where $B(\boldsymbol{r}) = B_u + B_p(\boldsymbol{r})$. Assuming the condition in Eq. (B4) is satisfied, Eq. (10) in the main text

$$\hat{H}_G(x,y)\psi^a_{\boldsymbol{k}}(x,y)=E^2\psi^a_{\boldsymbol{k}}(x,y) \tag{B5}$$

can be discretized as follows:

$$\begin{aligned}&\left(p+\frac{e}{c}A_u\right)^2\psi^a_{\boldsymbol{k}}(\boldsymbol{r})\\&=-\hbar^2\left(\frac{\psi^a_{\boldsymbol{k}}(\boldsymbol{r}+a\hat{\boldsymbol{x}})+\psi^a_{\boldsymbol{k}}(\boldsymbol{r}-a\hat{\boldsymbol{x}})-2\psi^a_{\boldsymbol{k}}(\boldsymbol{r})}{a^2}\right)\\&\quad-\hbar^2\left(\frac{\psi^a_{\boldsymbol{k}}(\boldsymbol{r}+a\hat{\boldsymbol{y}})+\psi^a_{\boldsymbol{k}}(\boldsymbol{r}-a\hat{\boldsymbol{y}})-2\psi^a_{\boldsymbol{k}}(\boldsymbol{r})}{a^2}\right)\\&\quad+\frac{e^2}{c^2}A_u^2\psi^a_{\boldsymbol{k}}(\boldsymbol{r})\\&\quad-\frac{i\hbar e}{c}A_{ux}\left(\frac{\psi^a_{\boldsymbol{k}}(\boldsymbol{r}+a\hat{\boldsymbol{x}})-\psi^a_{\boldsymbol{k}}(\boldsymbol{r}-a\hat{\boldsymbol{x}})}{a}\right)\\&\quad-\frac{i\hbar e}{c}A_{uy}\left(\frac{\psi^a_{\boldsymbol{k}}(\boldsymbol{r}+a\hat{\boldsymbol{y}})-\psi^a_{\boldsymbol{k}}(\boldsymbol{r}-a\hat{\boldsymbol{y}})}{a}\right)\end{aligned}$$

and

$$\begin{aligned}&\left(\frac{e^2}{c^2}A_p^2+\frac{2e}{c}\boldsymbol{A}_p\cdot\boldsymbol{p}\right)\psi^a_{\boldsymbol{k}}(\boldsymbol{r})\\&=\frac{e^2}{c^2}A_p^2\psi^a_{\boldsymbol{k}}(\boldsymbol{r})\\&\quad-\frac{i\hbar e}{c}A_{px}\left(\frac{\psi^a_{\boldsymbol{k}}(\boldsymbol{r}+a\hat{\boldsymbol{x}})-\psi^a_{\boldsymbol{k}}(\boldsymbol{r}-a\hat{\boldsymbol{x}})}{a}\right)\\&\quad-\frac{i\hbar e}{c}A_{py}\left(\frac{\psi^a_{\boldsymbol{k}}(\boldsymbol{r}+a\hat{\boldsymbol{y}})-\psi^a_{\boldsymbol{k}}(\boldsymbol{r}-a\hat{\boldsymbol{y}})}{a}\right).\end{aligned}$$

Now using these two expressions in the eigenvalue equation (10) and multiplying both sides with $\frac{-a^2}{\hbar^2}$, we get

$$\begin{aligned}\epsilon\psi^a_{\boldsymbol{k}}(\boldsymbol{r})&=\left[1+\frac{iea}{\hbar c}(A_{ux}+A_{px})\right]\psi^a_{\boldsymbol{k}}(\boldsymbol{r}+a\hat{\boldsymbol{x}})\\&\quad+\left[1-\frac{iea}{\hbar c}(A_{ux}+A_{px})\right]\psi^a_{\boldsymbol{k}}(\boldsymbol{r}-a\hat{\boldsymbol{x}})\\&\quad+\left[1+\frac{iea}{\hbar c}(A_{uy}+A_{py})\right]\psi^a_{\boldsymbol{k}}(\boldsymbol{r}+a\hat{\boldsymbol{y}})\\&\quad+\left[1-\frac{iea}{\hbar c}(A_{uy}+A_{py})\right]\psi^a_{\boldsymbol{k}}(\boldsymbol{r}-a\hat{\boldsymbol{y}})\\&\quad-\left[\frac{e^2}{\hbar^2c^2}a^2\left(A_u^2+A_p^2\right)\right.\\&\quad+\frac{2e^2a^2}{\hbar^2c^2}(A_{ux}A_{px}+A_{uy}A_{py})\\&\quad\left.+\frac{ea^2}{\hbar c}(B_u+B_p)+4\right]\psi^a_{\boldsymbol{k}}(\boldsymbol{r}),\end{aligned} \tag{B6}$$

where $\epsilon = \frac{-E^2a^2}{v_F^2\hbar^2}$ is the dimensionless energy. Now, as shown in Eq. (12), we have

$$\psi^a_{\boldsymbol{k}}(\boldsymbol{r})=\sum_i g(\boldsymbol{R}_i)w(\boldsymbol{r}-\boldsymbol{R}_i),$$

where $w(\boldsymbol{r}-\boldsymbol{R}_i) = \exp(-i\frac{e\boldsymbol{A}_u\cdot\boldsymbol{R}_i}{\hbar c})w_0(\boldsymbol{r}-\boldsymbol{R}_i)$ are the phase-transformed Wannier functions. Defining $\boldsymbol{R}_i - a\hat{\boldsymbol{x}} = \boldsymbol{R}_l$, from Eq. (B6) we get

$$\begin{aligned}&\epsilon\sum_l g(\boldsymbol{R}_l)w(\boldsymbol{r}-\boldsymbol{R}_l)\\&=\left[1+\frac{iea}{\hbar c}(A_{ux}+A_{px})\right]\sum_l g(\boldsymbol{R}_l+a\hat{\boldsymbol{x}})w(\boldsymbol{r}-\boldsymbol{R}_l)\\&\quad+\left[1-\frac{iea}{\hbar c}(A_{ux}+A_{px})\right]\sum_l g(\boldsymbol{R}_l-a\hat{\boldsymbol{x}})w(\boldsymbol{r}-\boldsymbol{R}_l)\\&\quad+\left[1+\frac{iea}{\hbar c}(A_{uy}+A_{py})\right]\sum_l g(\boldsymbol{R}_l+a\hat{\boldsymbol{y}})w(\boldsymbol{r}-\boldsymbol{R}_l)\\&\quad+\left[1-\frac{iea}{\hbar c}(A_{uy}+A_{py})\right]\sum_l g(\boldsymbol{R}_l-a\hat{\boldsymbol{y}})w(\boldsymbol{r}-\boldsymbol{R}_l)\\&\quad-\left[\frac{e^2}{\hbar^2c^2}a^2\left(A_u^2+A_p^2\right)+\frac{2e^2a^2}{\hbar^2c^2}(A_{ux}A_{px}+A_{uy}A_{py})\right.\\&\quad\left.+\frac{ea^2}{\hbar c}(B_u+B_p)+4\right]\sum_l g(\boldsymbol{R}_l)w(\boldsymbol{r}-\boldsymbol{R}_l).\end{aligned}$$

Now multiplying both sides of the above equation with $w^*(\boldsymbol{r}-\boldsymbol{R}_j)$ and using the orthogonality property of the phase-transformed Wannier functions (given later in this appendix), we finally get

$$\begin{aligned}\epsilon g(\boldsymbol{R}_j)&=\left[1+\frac{iea}{\hbar c}(A_{ux}+A_{px})\right]g(\boldsymbol{R}_j+a\hat{\boldsymbol{x}})\\&\quad+\left[1-\frac{iea}{\hbar c}(A_{ux}+A_{px})\right]g(\boldsymbol{R}_j-a\hat{\boldsymbol{x}})\\&\quad+\left[1+\frac{iea}{\hbar c}(A_{uy}+A_{py})\right]g(\boldsymbol{R}_j+a\hat{\boldsymbol{y}})\\&\quad+\left[1-\frac{iea}{\hbar c}(A_{uy}+A_{py})\right]g(\boldsymbol{R}_j-a\hat{\boldsymbol{y}})\\&\quad-\left[\frac{e^2}{\hbar^2c^2}a^2\left(A_u^2+A_p^2\right)\right.\\&\quad+\frac{2e^2a^2}{\hbar^2c^2}(A_{ux}A_{px}+A_{uy}A_{py})\\&\quad\left.+\frac{ea^2}{\hbar c}(B_u+B_p)+4\right]g(\boldsymbol{R}_j).\end{aligned} \tag{B7}$$

All the terms that are quadratic in vector potential can be ignored under the condition (B4) in the above equation. This finally gives us Eq. (13), which is the famous Hofstadter-Harper equation. Now, for the proof of orthogonality of phase-transformed Wannier functions, we proceed as follows:

$$\begin{aligned} I &= \int w^*(\boldsymbol{r}-\boldsymbol{R}_j)w(\boldsymbol{r}-\boldsymbol{R}_l)\boldsymbol{dr} \\ &= \int e^{\frac{ie}{\hbar c}A_u(\boldsymbol{r})\cdot(\boldsymbol{R}_j-\boldsymbol{R}_l)}[w^0(\boldsymbol{r}-\boldsymbol{R}_j)]^* \\ &\quad\times w^0(\boldsymbol{r}-\boldsymbol{R}_l)\boldsymbol{dr} \\ &= \int e^{\frac{ie}{2\hbar c}(-B_u y\hat{\boldsymbol{x}}+B_u x\hat{\boldsymbol{y}})\cdot[(m-m')a\hat{\boldsymbol{x}}+(n-n')a\hat{\boldsymbol{y}}]} \\ &\quad\times[w^0(\boldsymbol{r}-\boldsymbol{R}_j)]^* w^0(\boldsymbol{r}-\boldsymbol{R}_l)\boldsymbol{dr} \\ &= \int e^{-\frac{ie}{2\hbar c}B_u y(m-m')a}e^{-\frac{ie}{2\hbar c}B_u x(n-n')a} \\ &\quad\times[w^0(x-ma,y-na)]^* \\ &\quad\times w^0(x-m'a,y-n'a)\boldsymbol{dr}, \end{aligned}$$

which can further be simplified as

$$\begin{aligned} I &= \int e^{-\frac{ie}{2\hbar c}B_u y(m-m')a}e^{-\frac{ie}{2\hbar c}B_u x(n-n')a} \\ &\quad\times[w^0(x-ma)]^*[w^0(y-na)]^* \\ &\quad\times w^0(x-m'a)w^0(y-n'a)dxdy \\ &= \int e^{-\frac{ie}{2\hbar c}B_u x(n-n')a}[w^0(x-ma)]^*w^0(x-m'a)dx \\ &\quad\times\int e^{-\frac{ie}{2\hbar c}B_u y(m-m')a}[w^0(y-na)]^*w^0(y-n'a)dy. \end{aligned}$$

Now, for x integration, the y coordinate does not change; hence, $n-n'=0$. Similarly, for y integration $m-m'=0$, which leads to

$$\begin{aligned} I &= \int [w^0(x-ma)]^*w^0(x-m'a)dx \\ &\quad\times\int [w^0(y-na)]^*w^0(y-n'a)dy. \end{aligned}$$

Now we are left with Wannier functions in the absence of any magnetic field, which are orthonormal. Hence, we write

$$\begin{aligned} I &= \int [w^0(x-ma)]^*w^0(x-m'a)dx \\ &\quad\times\int [w^0(y-na)]^*w^0(y-n'a)dy \\ &= \delta_{mm'}\delta_{nn'} \end{aligned}$$

APPENDIX C: QUANTIZATION OF HALL CONDUCTIVITY IN TERMS OF THE TOPOLOGICAL INVARIANT

The following discussion is mostly available in Ref. [41]. We provide an abridged version. In the main text, using Eq. (16) in Eq. (8) gives

$$\hat{H}(k_x,k_y)u'_{k_x,k_y}=Eu'_{k_x,k_y},$$

where

$$\hat{H}(k_x,k_y)=\begin{bmatrix}0 & H_{12}\\ H_{21} & 0\end{bmatrix},$$

with

$$\begin{aligned} H_{12} &= \bigg[\left(-i\hbar\frac{\partial}{\partial x}+\hbar k_x+\frac{eA_x}{c}\right) \\ &\quad - i\left(-i\hbar\frac{\partial}{\partial y}+\hbar k_y+\frac{eA_y}{c}\right)\bigg] \end{aligned}$$

and

$$\begin{aligned} H_{21} &= \bigg[\left(-i\hbar\frac{\partial}{\partial x}+\hbar k_x+\frac{eA_x}{c}\right) \\ &\quad + i\left(-i\hbar\frac{\partial}{\partial y}+\hbar k_y+\frac{eA_y}{c}\right)\bigg]. \end{aligned}$$

Here A_x and A_y depict the x and y components of the total vector potential $\boldsymbol{A}(\boldsymbol{r})$ given in the main text. We write the Hall conductance for a completely filled band (here we perform the calculation for a single band; hence, the band index does not appear) as

$$\begin{aligned} \sigma_{xy} &= \frac{e^2}{h}\frac{1}{2\pi i}\int d^2k\int d^2r\bigg(\frac{\partial u'^*_{k_x,k_y}}{\partial k_y}\frac{\partial u'_{k_x,k_y}}{\partial k_x} \\ &\quad - \frac{\partial u'^*_{k_x,k_y}}{\partial k_x}\frac{\partial u'_{k_x,k_y}}{\partial k_y}\bigg), \end{aligned}$$

where the integrations are taken over the unit cells in r and k space. The above equation is the same as the Eq. (17) but written explicitly in terms of the components. In Eq. (17), the Hall conductivity is written as a curl of a function that is a function of Bloch vectors, and the integration is over the magnetic Brillouin zone, which has the topology of a torus. Thus, Eq. (17) can be written equivalently (using Stoke's law) as

$$\sigma_{xy}=\frac{e^2}{h}\frac{1}{2\pi i}\int_{\partial MBZ}\boldsymbol{dk}\cdot\hat{\boldsymbol{A}}(k_x,k_y), \tag{C1}$$

where the integration is over the boundary of the MBZ. Since the torus has no boundary, if $\hat{\boldsymbol{A}}(k_x,k_y)$ is uniquely defined on the entire torus, it yields $\sigma_{xy}=0$. Thus, a finite Hall conductivity implies that the function $\hat{\boldsymbol{A}}(k_x,k_y)$ cannot be uniquely defined in this space. Now, to understand the nontrivial topology of $\hat{\boldsymbol{A}}(k_x,k_y)$, we consider the gauge transformation

$$\begin{bmatrix}u^{aa}_{k_x,k_y}\\ u^{bb}_{k_x,k_y}\end{bmatrix}=e^{if(k_x,k_y)}\begin{bmatrix}u^{a}_{k_x,k_y}\\ u^{b}_{k_x,k_y}\end{bmatrix}, \tag{C2}$$

where $f(k_x,k_y)$ is some arbitrary smooth function of only k_x and k_y. We can see that this transformation changes the phase of the wave function but leaves the physical quantity like the Hall conductivity invariant. Now, as u'_{k_x,k_y} vanishes for some (k_x,k_y) in the torus (magnetic Bloch functions have zeros), the transformation given by Eq. (C2) cannot be defined over the entire MBZ uniquely. Let us consider the simplest case of a single zero of u'_{k_x,k_y} in the MBZ. We divide the MBZ into two regions using a circular boundary such that the inside region (say, region I) has a zero of the function $u'_{k_x,k_y}(x,y)$, say, $\boldsymbol{k} = \boldsymbol{k}_0$, and the outside region (say, region II) does not have a zero. Thus, for region I, we define some other function u''_{k_x,k_y} which is nonzero everywhere in this region. Hence, for region I, say, H_I, we can write

$$\begin{bmatrix} u^{a1}_{k_x,k_y} \\ u^{b1}_{k_x,k_y} \end{bmatrix} = e^{ig(k_x,k_y)} \begin{bmatrix} u^{a}_{k_x,k_y} \\ u^{b}_{k_x,k_y} \end{bmatrix},$$

and for region II, say, H_{II}, we can have

$$\begin{bmatrix} u^{a2}_{k_x,k_y} \\ u^{b2}_{k_x,k_y} \end{bmatrix} = e^{ih(k_x,k_y)} \begin{bmatrix} u^{a}_{k_x,k_y} \\ u^{b}_{k_x,k_y} \end{bmatrix}.$$

Equation (17) in the main text now becomes

$$\sigma_{xy} = \frac{e^2}{h}\frac{1}{2\pi i}\left\{ \int_{H_1} d^2k[\nabla \times \hat{\boldsymbol{A}}^1(k_x,k_y)]_3 + \int_{H_2} d^2k[\nabla \times \hat{\boldsymbol{A}}^2(k_x,k_y)]_3 \right\}, \tag{C3}$$

where the vectors $\hat{\boldsymbol{A}}^1(k_x,k_y)$ and $\hat{\boldsymbol{A}}^2(k_x,k_y)$ are defined for regions I and II, respectively, and can be explicitly written as

$$\hat{\boldsymbol{A}}^1(k_x,k_y) = \int d^2r\Bigg[\hat{\boldsymbol{k}}_x\left(i\frac{\partial g}{\partial k_x}u^{a*}_{k_x,k_y}u^{a}_{k_x,k_y} + i\frac{\partial g}{\partial k_x}u^{b*}_{k_x,k_y}u^{b}_{k_x,k_y} + u^{a*}_{k_x,k_y}\frac{\partial}{\partial k_x}u^{a}_{k_x,k_y} + u^{b*}_{k_x,k_y}\frac{\partial}{\partial k_x}u^{b}_{k_x,k_y}\right) + \hat{\boldsymbol{k}}_y\left(i\frac{\partial g}{\partial k_y}u^{a*}_{k_x,k_y}u^{a}_{k_x,k_y} + i\frac{\partial g}{\partial k_y}u^{b*}_{k_x,k_y}u^{b}_{k_x,k_y} + u^{a*}_{k_x,k_y}\frac{\partial}{\partial k_y}u^{a}_{k_x,k_y} + u^{b*}_{k_x,k_y}\frac{\partial}{\partial k_y}u^{b}_{k_x,k_y}\right)\Bigg] \tag{C4}$$

and

$$\hat{\boldsymbol{A}}^2(k_x,k_y) = \int d^2r\Bigg[\hat{\boldsymbol{k}}_x\left(i\frac{\partial h}{\partial k_x}u^{a*}_{k_x,k_y}u^{a}_{k_x,k_y} + i\frac{\partial h}{\partial k_x}u^{b*}_{k_x,k_y}u^{b}_{k_x,k_y} + u^{a*}_{k_x,k_y}\frac{\partial}{\partial k_x}u^{a}_{k_x,k_y} + u^{b*}_{k_x,k_y}\frac{\partial}{\partial k_x}u^{b}_{k_x,k_y}\right) + \hat{\boldsymbol{k}}_y\left(i\frac{\partial h}{\partial k_y}u^{a*}_{k_x,k_y}u^{a}_{k_x,k_y} + i\frac{\partial h}{\partial k_y}u^{b*}_{k_x,k_y}u^{b}_{k_x,k_y} + u^{a*}_{k_x,k_y}\frac{\partial}{\partial k_y}u^{a}_{k_x,k_y} + u^{b*}_{k_x,k_y}\frac{\partial}{\partial k_y}u^{b}_{k_x,k_y}\right)\Bigg]. \tag{C5}$$

Here we have used $u^a_{k_x,k_y}$ and $u^b_{k_x,k_y}$ for the normalized eigenfunctions. From (C4) and (C5), we get

$$\hat{\boldsymbol{A}}^1(k_x,k_y) - \hat{\boldsymbol{A}}^2(k_x,k_y) = 2i\nabla_{\boldsymbol{k}}t(\boldsymbol{k}), \tag{C6}$$

where $t(\boldsymbol{k}) = g(\boldsymbol{k}) - h(\boldsymbol{k})$. We now write, using Stokes's theorem and the fact that the two regions have opposite directions for circulation, Eq. (C3) as

$$\sigma_{xy} = \frac{e^2}{h}\frac{1}{2\pi i}\int_C \boldsymbol{dk}\cdot[\hat{\boldsymbol{A}}^1(k_x,k_y) - \hat{\boldsymbol{A}}^2(k_x,k_y)],$$

which on using Eq. (C6) leads to

$$\sigma_{xy} = \frac{2e^2}{h}\frac{1}{2\pi}\int_C \boldsymbol{dk}\cdot\nabla_{\boldsymbol{k}}t(\boldsymbol{k}),$$

where C denotes a closed boundary between the two regions. At each point on the closed loop C, the wave function has to be single valued; therefore, after traversing the complete loop C the two wave functions should still have the same phase relationship. This is possible only if

$$\begin{bmatrix} u^{a2}_{k_x,k_y} \\ u^{b2}_{k_x,k_y} \end{bmatrix} = e^{i[t(k_x,k_y)+2\pi\sigma_H]} \begin{bmatrix} u^{a1}_{k_x,k_y} \\ u^{b1}_{k_x,k_y} \end{bmatrix},$$

where σ_H is an integer. This expression finally comes out to be

$$\sigma_{xy} = \frac{2e^2}{h}\sigma_H,$$

where σ_H is an integer. Here the factor of 2 comes from the sublattice degrees of freedom.

APPENDIX D: DIOPHANTINE EQUATION

The integral in Eq. (C1) is actually the Berry phase/gauge-invariant geometric phase accumulated by the wave function in the reciprocal space [7]

$$\gamma = \oint_C \boldsymbol{dk}\cdot\hat{\boldsymbol{A}}(k_x,k_y).$$

Written explicitly over the contour defined in Fig. 5

$$\gamma = \int_{C_1} dk_x \int\left[u^{a*}_{k_x,k_y}\frac{\partial u^a{}_{k_x,k_y}}{\partial k_x} + u^{b*}_{k_x,k_y}\frac{\partial u^b{}_{k_x,k_y}}{\partial k_x}\right]dxdy + \int_{C_2} dk_y \int\left[u^{a*}_{k_x,k_y}\frac{\partial u^a{}_{k_x,k_y}}{\partial k_y} + u^{b*}_{k_x,k_y}\frac{\partial u^b{}_{k_x,k_y}}{\partial k_y}\right]dxdy$$

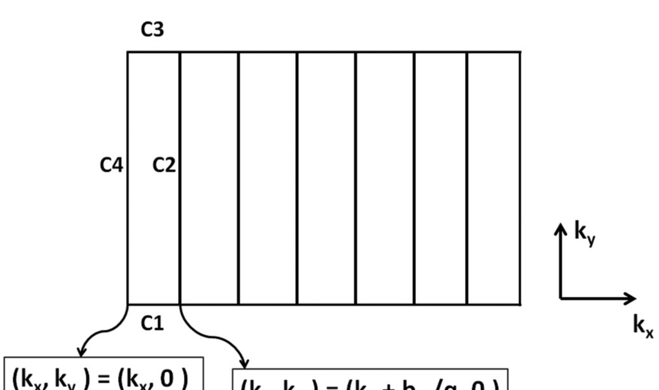

FIG. 5. Magnetic Brillouin zone.

$$+\int_{C_3} dk_x \int \left[u^{a*}_{k_x,k_y} \frac{\partial u^a{}_{k_x,k_y}}{\partial k_x} + u^{b*}_{k_x,k_y} \frac{\partial u^b{}_{k_x,k_y}}{\partial k_x} \right] dxdy$$
$$+\int_{C_4} dk_y \int \left[u^{a*}_{k_x,k_y} \frac{\partial u^a{}_{k_x,k_y}}{\partial k_y} + u^{b*}_{k_x,k_y} \frac{\partial u^b{}_{k_x,k_y}}{\partial k_y} \right] dxdy, \tag{D1}$$

where we take one of the MBZs out of the following. Even though the integral defined in Eq. (C1) is a gauge-invariant quantity, the Berry connection $\boldsymbol{A}$ is not unique. To fix it the following construction for parallel transportation [53] is made:

$$\int u^*_{k_x,k_y} \frac{\partial u_{k_x}, k_y}{\partial k_y} dxdy = 0 \tag{D2}$$

and

$$\int u^*_{k_x,0} \frac{\partial u_{k_x,0}}{\partial k_x} dxdy = 0. \tag{D3}$$

Equation (D2) renders the second and fourth terms in expression (D1) to zero, and Eq. (D3) makes the contribution from the first term zero [54]. This contribution makes the phases of the wave function satisfy

$$u_{k_x+\frac{b_1}{q},k_y} = u_{k_x,k_y}, \tag{D4}$$

$$u_{k_x,k_y+b_2} = e^{i\delta(k_x)} u_{k_x,k_y}, \tag{D5}$$

where $\delta(k_x)$ is the k_x-dependent phase factor. The total phase change around the MBZ therefore needs to satisfy

$$i\delta\left(k_x + \frac{b_1}{q}\right) - i\delta(k_x) = 2\pi i \times \text{integer}. \tag{D6}$$

Considering the contribution from both sublattices, we can therefore write

$$\int_{\partial MBZ} \boldsymbol{dk} \cdot \hat{\boldsymbol{A}}(k_x, k_y) = 4\pi i \times \text{integer}.$$

However, from the Kubo formula it was also shown that

$$\int_{\partial MBZ} \boldsymbol{dk} \cdot \hat{\boldsymbol{A}}(k_x, k_y) = 4\pi i \sigma_H.$$

Thus, we can identify this integer as σ_H, which enables us to write Eq. (D6) as

$$\delta\left(k_x + \frac{b_1}{q}\right) = \delta(k_x) + 2\pi\sigma_H. \tag{D7}$$

The boundary conditions (D4) and (D5) along with Eq. (D7) can now be used to set the following conditions on magnetic Bloch functions ψ_{k_x,k_y} (or $\psi_{\boldsymbol{k}}$) [44,45] given in the main text, namely,

$$\psi_{k_x+\frac{b_1}{q},k_y} = \psi_{k_x,k_y}, \tag{D8}$$

$$\psi_{k_x,k_y+b_2} = e^{i\sigma_H k_x q a} \psi_{k_x,k_y}. \tag{D9}$$

But the magnetic Bloch functions, being eigenstates of the magnetic translational operator [defined in Eq. (9)], also obey the group properties of the magnetic translational group [given in Eqs. (14)]. Using them, we get

$$M(qa\hat{\boldsymbol{x}})\psi_{\boldsymbol{k}} = e^{i\boldsymbol{k}\cdot qa\hat{\boldsymbol{x}}} \psi_{\boldsymbol{k}}, \tag{D10}$$

$$M(a\hat{\boldsymbol{y}})\psi_{\boldsymbol{k}} = e^{i\boldsymbol{k}\cdot a\hat{\boldsymbol{y}}} \psi_{\boldsymbol{k}}, \tag{D11}$$

and

$$\begin{aligned} M_{\boldsymbol{R}_1} M_{\boldsymbol{R}_2} \psi_{\boldsymbol{k}} &= M_{\boldsymbol{R}_2} M_{\boldsymbol{R}_1} e^{2\pi i \frac{p}{q}} \psi_{\boldsymbol{k}} \\ &= M_{\boldsymbol{R}_2} e^{2\pi i \frac{p}{q}} M_{\boldsymbol{R}_1} \psi_{\boldsymbol{k}} \\ &= M_{\boldsymbol{R}_2} e^{2\pi i \frac{p}{q}} e^{i\boldsymbol{k}.a\hat{\boldsymbol{y}}} \psi_{\boldsymbol{k}} \\ &= e^{i(\boldsymbol{k}+\frac{p}{q}\boldsymbol{b}_2).a\hat{\boldsymbol{y}}} M_{\boldsymbol{R}_2} \psi_{\boldsymbol{k}}, \end{aligned} \tag{D12}$$

where $\boldsymbol{R}_1 = a\hat{\boldsymbol{y}}$ and Eq. (D11) is being used. Also for $\boldsymbol{R}_2 = a\hat{\boldsymbol{x}}$, we can write Eq. (D12) as

$$M_{a\hat{\boldsymbol{y}}} M_{a\hat{\boldsymbol{x}}} \psi_{\boldsymbol{k}} = e^{i(\boldsymbol{k}+\frac{p}{q}\boldsymbol{b}_2)\cdot a\hat{\boldsymbol{y}}} M_{a\hat{\boldsymbol{x}}} \psi_{\boldsymbol{k}},$$

where $M(a\hat{\boldsymbol{x}})\psi_{\boldsymbol{k}}$ depicts the eigenfunction of $M(a\hat{\boldsymbol{y}})$ with the eigenvalue $e^{i(\boldsymbol{k}+\frac{p}{q}\boldsymbol{b}_2)\cdot a\hat{\boldsymbol{y}}}$. Similarly, $M(2a\hat{\boldsymbol{x}})\psi_{\boldsymbol{k}}$, $M(3a\hat{\boldsymbol{x}})\psi_{\boldsymbol{k}}$, $M(4a\hat{\boldsymbol{x}})\psi_{\boldsymbol{k}}, \ldots$ depict eigenfunctions of $M(a\hat{\boldsymbol{y}})$ with eigenvalues $e^{i(\boldsymbol{k}+\frac{2p}{q}\boldsymbol{b}_2)\cdot a\hat{\boldsymbol{y}}}$, $e^{i(\boldsymbol{k}+\frac{3p}{q}\boldsymbol{b}_2)\cdot a\hat{\boldsymbol{y}}}$, $e^{i(\boldsymbol{k}+\frac{4p}{q}\boldsymbol{b}_2)\cdot a\hat{\boldsymbol{y}}}$, ..., respectively. These functions, being degenerate with $\psi_{\boldsymbol{k}}$, have the same energy eigenvalues for the Hamiltonian in Eq. (8). Hence, corresponding to each energy eigenvalue, we have q degenerate states depicting the q-fold degeneracy of the system. Therefore, we can write [44]

$$M(a\hat{\boldsymbol{x}})\psi_{\boldsymbol{k}} = e^{i\mu\boldsymbol{k}\cdot qa\hat{\boldsymbol{x}}} \psi_{\boldsymbol{k}+\frac{p}{q}\boldsymbol{b}_2}.$$

Here μ is an integer (for the significance of μ see [55]). Now applying $M(a\hat{\boldsymbol{x}})$ q times to the above equation, we get

$$M(qa\hat{\boldsymbol{x}})\psi_{k_x,k_y} = e^{i\mu q\boldsymbol{k}\cdot qa\hat{\boldsymbol{x}}} \psi_{k_x,k_y+pb_2},$$

which on using Eqs. (D9) and (D10) becomes

$$e^{i\boldsymbol{k}\cdot qa\hat{\boldsymbol{x}}} \psi_{k_x,k_y} = e^{i\mu q\boldsymbol{k}\cdot qa\hat{\boldsymbol{x}}} e^{ip\sigma_H \boldsymbol{k}\cdot qa\hat{\boldsymbol{x}}} \psi_{k_x,k_y}.$$

This gives

$$\mu q + \sigma_H p = 1,$$

which is the Diophantine equation to calculate quantum Hall integers [33] for bands in the energy spectrum.

[1] K. V. Klitzing, G. Dorda, and M. Pepper, Phys. Rev. Lett. **45**, 494 (1980).

[2] D. C. Tsui, H. L. Stormer, and A. C. Gossard, Phys. Rev. Lett. **48**, 1559 (1982).

[3] R. B. Laughlin, Phys. Rev. B **23**, 5632 (1981).

[4] B. I. Halperin, Phys. Rev. B **25**, 2185 (1982).

[5] K. S. Novoselov, A. K. Geim, S. V. Morozov, D. Jiang, M. I. Katnelson, I. V. Grigorieva, S. V. Dubonos, and A. A. Firsov, Nature (London) **438**, 197 (2005).

[6] Y. Zhang, Y.-W. Tan, H. L. Stormer and P. Kim, Nature (London) **438**, 201 (2005).
[7] D. J. Thouless, M. Kohmoto, M. P. Nightingale, and M. den Nijs, Phys. Rev. Lett. **49**, 405 (1982).
[8] R. D. Hofstadter, Phys. Rev. B **14**, 2239 (1976).
[9] J. E. Avron, R. Seiler, and B. Simon, Phys. Rev. Lett. **51**, 51 (1983).
[10] F. D. M. Haldane, Phys. Rev. Lett. **61**, 2015 (1988).
[11] C. L. Kane and E. J. Mele, Phys. Rev. Lett. **95**, 226801 (2005).
[12] B. A. Bernevig, T. A. Hughes, and S. C. Zhang, Science, **314**, 1757 (2006).
[13] M. Z. Hasan and C. L. Kane, Rev. Mod. Phys. **82**, 3045 (2010).
[14] J. Zak, Phys. Rev. **134**, A1607 (1964).
[15] H. J. Fischbeck, Phys. Status Solidi **38**, 11 (1970).
[16] W. Florek, Acta Phys. Pol. A **92**, 399 (1997).
[17] A Matulis, F. M. Peeters, and P. Vasilopoulos, Phys. Rev. Lett. **72**, 1518 (1994).
[18] A. Krakovsky, Phys. Rev. B **53**, 8469 (1996).
[19] I. S. Ibrahim and F. M. Peeters, Phys. Rev. B **52**, 17321 (1995).
[20] M. C. Chang and Q. Niu, Phys. Rev. B **50**, 10843 (1994).
[21] G.-Y. Oh, Phys. Rev. B **60**, 1939 (1999).
[22] X. F. Wang, P. Vasilopoulos, and F. M. Peeters, Phys. Rev. B **70**, 155312 (2004).
[23] A. De Martino, L. Dell'Anna, and R. Egger, Phys. Rev. Lett. **98**, 066802 (2007).
[24] A. Nogaret, J. Phys. Condens. Matter **22**, 253201 (2010).
[25] N. Agrawal (Garg), S. Ghosh, and M. Sharma, Int. J. Mod. Phys. B, **27**, 1341003 (2013).
[26] P. D. Ye, D. Weiss, K. von Klitzing, K. Eberl, and H. Nickel, Appl. Phys. Lett. **67**, 1441 (1995).
[27] S. D. Bader, Rev. Mod. Phys. **78**, 1 (2006).
[28] M. Taillefumier, V. K. Dugaev, B. Canals, C. Lacroix, and P. Bruno, Phys. Rev. B **78**, 155330 (2008).
[29] I. Snyman, Phys. Rev. B **80**, 054303 (2009).
[30] W. Beugeling, N. Goldman, and C. M. Smith, Phys. Rev. B **86**, 075118 (2012).
[31] E. Brown, in *Solid State Physics: Advances in Research and Applications*, edited by F. Seitz, D. Turnbull, and H. Ehrenreich (Academic Press, New York and London, 1968), Vol. 22, pp. 353–354.
[32] J. Zak, Phys. Rev. **139**, A1159 (1965).
[33] I. I. Satija, *Butterfly in the Quantum World: The Story of the Most Fascinating Quantum Fractal* (Morgan and Claypool, San Rafael, CA, 2016), p. 10-3.
[34] J. M. Luttinger, Phys. Rev. **84**, 814 (1951).
[35] G. H. Wannier and D. R. Fredkin, Phys. Rev. **125**, 1910 (1962).
[36] S. Janecek, M. Aichinger, and E. R. Hernandez, Phys. Rev. B **87**, 235429 (2013).
[37] M. Governale and C. Ungarelli, Phys. Rev. B **58**, 7816 (1998).
[38] E. Brown, Phys. Rev. **133**, A1038 (1964).
[39] E. Muñoz, Z. Barticevic, and M. Pacheco, Phys. Rev. B **71**, 165301 (2005).
[40] Y. Hasegawa and M. Kohmoto, Phys. Rev. B **74**, 155415 (2006).
[41] M. Kohmoto, Ann. Phys. (NY) **160**, 343 (1984).
[42] C. H. Park, Y. W. Son, L. Yang, M. L. Cohen, and S. G. Louie, Phys. Rev. Lett. **103**, 046808 (2009).
[43] L. Brey and H. A. Fertig, Phys. Rev. Lett. **103**, 046809 (2009).
[44] I. Dana, Y. Avron, and J. Zak, J. Phys. C **18**, L679 (1985).
[45] M. Wilkinson, J. Phys.: Condens. Matter **10**, 7407 (1998).
[46] J. E. Avron, O. Kenneth, and G. Yehoshua, J. Phys. A **47**, 185202 (2014).
[47] R. Rammal, J. Phys. (Paris) **46**, 1345 (1985).
[48] R. R. Gerhardts, D. Pfannkuche, and V. Gudmundsson, Phys. Rev. B **53**, 9591 (1996).
[49] G. Gumbs, D. Miessein, and D. Huang, Phys. Rev. B **52**, 14755 (1995).
[50] J. E. Müller, Phys. Rev. Lett. **68**, 385 (1992).
[51] A. K. Geim and I. V. Grigorieva, Nature (London) **499**, 419 (2013).
[52] J. G. Park, J. Phys. Condens. Matter **28**, 301001 (2016).
[53] D. J. Thouless, J. Phys. C **17**, L325 (1984).
[54] D. Xiao, M.-C. Chang, and Q. Niu, Rev. Mod. Phys. **82**, 1959 (2010).
[55] H. Aoki and Y. Hatsugai, Phys. Rev. B **90**, 045206 (2014).